

Feasibility Study for Real Time Three Dimensional Doppler Intracardiac Echocardiography

Edward D. Light¹, Salim F. Idriss², Warren Lee¹, Patrick D. Wolf¹ and Stephen W. Smith¹

¹Department of Biomedical Engineering, Duke University, Durham, NC 27708
email:edl@duke.edu

²Department of Pediatrics, Duke University Medical Center, Durham, NC 27708

Using catheter mounted two-dimensional array transducers, we have obtained real-time three-dimensional Color Flow and Spectral Doppler ultrasound images in phantoms. We have constructed several transducers operating at 5 MHz with up to 137 channels inside a 12 French catheter lumen. The transducer configuration may be side scanning or beveled with respect to the long axis of the catheter lumen. We have also included six electrodes to acquire simultaneous electrocardiograms. We have measured Doppler signals in two phantoms, a string phantom and a pulsatile flow phantom. Using an open chest sheep model, we inserted the catheter into the cardiac chambers to study the utility of *in vivo* 3D intracardiac Doppler echocardiography.

Key Words: 2D array transducer; Catheter; Doppler imaging; Intracardiac echocardiography; Real time volumetric imaging

Short title: Real Time 3D Doppler ICE

Introduction

There has been much interest in Intracardiac Echocardiography (ICE) for monitoring interventional procedures such as electrophysiological (EP) techniques and minimally invasive surgery. This technology is dependent upon placing the ultrasound transducer inside a catheter. By placing the catheter within the cardiac chambers, several of the challenges of transthoracic transducers can be overcome. With a total scanning depth of up to 8 cm for an intracardiac transducer, higher frequency transducers can be employed to improve spatial resolution.

The extensive research literature in ICE has recently been reviewed in articles by Kalman et al.¹ and Bruce et al.² who described applications including direct visualization of cardiac anatomy, evaluation of the accuracy of catheter tip placement, and measurement of lesion size and location from radio frequency (RF) ablation. ICE may also lead to clinical benefits by improving guidance during technically difficult procedures such as transseptal puncture and coronary sinus access. This may have the additional advantage of reduced fluoroscopic exposure to patient and medical personnel.

Current commercial ICE systems include two technologies: (1) a mechanical system that uses a 9 MHz rotating ultrasound transducer to produce a 360° scan perpendicular to the long axis of a 9 F catheter (EP Technologies, Boston Scientific, San Jose CA); (2) a

phased array system that uses a 64 channel linear array transducer operating at a center frequency of 8 MHz to produce a sector scan parallel to the long axis of a 10 F catheter (Acuson Corporation, Mountain View, CA). The Acuson system features Color Flow, Spectral and Continuous Wave Doppler capabilities.³

We have previously described real time three dimensional ultrasound imaging⁴⁻⁶ using 2D array transducers operating from 2-10 MHz.^{7,8,9} Clinical and animal evaluations for cardiac applications have shown potential advantages over conventional 2D scanners for measurement of ventricular volumes,^{10,11} reduced scanning times in dobutamine stress echo exams¹² and guidance of right ventricular endomyocardial biopsy.¹³ Researchers have also shown that using real time 3D color Doppler improves the measurement of peak left ventricular flow velocities.¹⁴

We have demonstrated real time 3D ICE and shown images with the catheter based 2D array transducers we developed.^{7, 15-18} Using these catheter array transducers, we measured spatial resolution of 2 mm at a depth of 2 cm in the real time 3D scans. We described preliminary images of cardiac anatomy using real time 3D ICE in the *in vivo* sheep model including all four chambers and valves as well as 3D imaging of *in vitro* cardiac RF ablation. The purpose of this paper is to report on our study to 1) test the feasibility of our catheter based 2D array transducers to obtain 3D Doppler images when used with a real time 3D scanner (Model 1, Volumetrics Medical Imaging, Durham, NC), 2) test the accuracy of the Doppler data with a simple string phantom, and 3) obtain *in vivo* 3D Doppler images in a sheep model.

Methods

Volumetric Scanner System

The commercial Volumetrics Medical Imaging ultrasound scanner generates a real time 3D pyramidal scan using as many as 512 transmitters and up to 256 receive channels. The scanner uses 16:1 receive mode parallel receive processing to generate 4100 B-mode image lines at up to 60 volumes per second. Figure 1 shows a schematic of the catheter mounted matrix array producing the pyramidal scan with two simultaneous orthogonal B-mode image planes (perpendicular to the transducer array) and two C-mode planes (parallel to the array). The transducer is shown mounted at a 30° angle compared to the long axis of the catheter lumen. Each image plane can also be inclined at any desired angle. By integrating and spatially filtering between two user selected planes, e.g. the C-mode planes, the system also displays real time 3D rendered images. The commercial system features 2D arrays transthoracic transducers operating at 2.5 and 3.5 MHz. It also includes real time volumetric Spectral Doppler and Color Flow Doppler imaging capabilities with a specified accuracy of $\pm 10\%$ for velocities between 25 and 300 cm/s.¹⁹

Transducer fabrication

We used two different catheter transducers, operating at 5 MHz, in this feasibility study 1) a 13 x 11 array including 64 active channels in a 12 French catheter (O.D. = 3.8 mm) and 2) a 13 x 13 array with 137 active elements in a 12 French catheter lumen. Both transducers were constructed on a multi-layer flex circuit as previously described.^{8, 15}

The first transducer is mounted within the catheter at a 30° bevel with respect to the long axis of the catheter. The second transducer used a ribbon based cable (W.L. Gore & Associates) to enable 137 channels to fit in the lumen.²⁰ While the tip of this catheter is a 12 French lumen, the body of the catheter is actually an 8 French lumen (O.D. = 2.6mm). The need for a 12 French tip is determined by the size of our flex circuit. Figure 2 shows a photograph of the 12 F, 137 element array on its flex circuit.

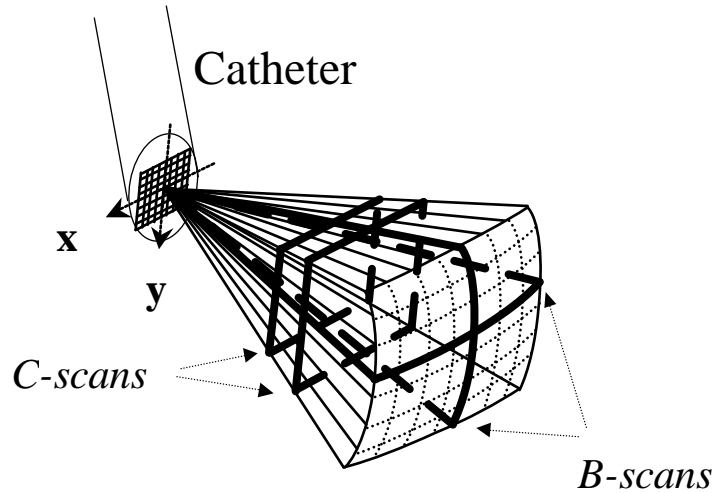


Figure 1: Schematic of the pyramidal scan from catheter matrix array. The transducer is shown at a 30° angle compared to the long axis of the catheter, at an enlarged scale. Bold lines indicate possible display planes. By integrating and spatially filtering between two user selected planes, real time 3D rendered images are displayed.



Figure 2: Photograph of the 12 F, 137 element flex circuit.

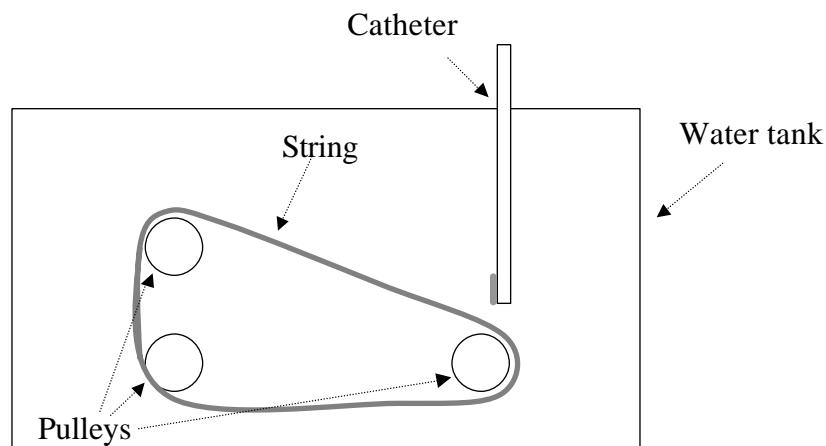


Figure 3: Schematic of the string phantom. One of the pulleys is motor driven.

Phantoms

We used two phantoms to evaluate our system. The first phantom is a moving string phantom consisting of a string rotating around three pulleys, as shown in figure 3. One of

the pulleys is motor driven. The string has a mark on it and is of known length so that we could visually measure its velocity and compare that to the ultrasound data. The second phantom simulated a cardiac jet, and is shown schematically in figure 4. It consists of a pulsatile pump and a 7.3 mm diameter orifice in a rubber stopper at the end of a tube. The fluid was allowed to collect in a reservoir. A suspension of corn starch in water was used as a blood mimicking fluid.

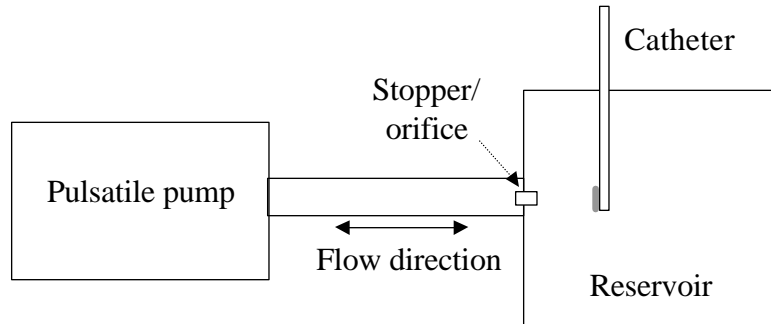


Figure 4: Schematic of the pulsatile pump phantom.

We used the 12 French catheter with 64 elements with the string phantom to measure the speed of the string at three different velocities using both Spectral Doppler and Color Flow. We measured the speed with a stop watch and a mark on the string. Two independent observers measured the rate 3 times each and they were averaged for each velocity. Fifteen total velocities were measured. To get a measurement while using Color Flow, we used the color marker and chose the velocity where the largest amount of the volume was marked with the marker. For each Doppler imaging technique, we measured the maximum string velocities before we saw aliasing. The same catheter was used to image the jet phantom.

Statistics

To obtain our graphs, the data were exported into Matlab (The MathWorks, Natick, MA). Plots of the Doppler results versus the observed data were generated for both Spectral Doppler and Color Flow. A line was fitted using the least squares method with the polyfit function. An error line was also generated for each plot using the polyval function.

Doppler imaging

For CF Doppler, the machine was set so that the wall filter was maximized, the minimum velocity was set to 0, the CF reject was 7, the burst length was 3 to prevent the small 2D elements from heating, PRF 6.2 kHz.

For the Spectral Doppler the compression was set to 50%, gate width was 4 mm, Spectral reject was 0, the base line was shifted down to 0, the burst length was 3 and the PRF was 6.2 kHz.

Animal model

A single sheep was used in this study approved by the Institutional Animal Care and Use Committee at Duke University conforming to the Research Animal Use Guidelines of the

American Heart Association. Anesthesia was induced with ketamine hydrochloride, 15-22 mg/kg IM, and maintained with isoflurane gas, 1-5%, delivered through a nose cone. After peripheral IV access was obtained, the animal was placed on its left side on a water heated thermal pad. A tracheotomy was performed and the animal was mechanically ventilated with 95-99% oxygen. To prevent rumenal typany, a nasogastric tube was passed into the stomach. A femoral arterial line was placed on the left side via a percutaneous puncture. Electrolyte and respirator adjustments were made based on serial electrolyte and arterial blood gas measurements. An IV maintenance fluid with 0.9% sodium chloride was infused continuously. Blood pressure, lead II electrocardiogram, and temperature were continuously monitored throughout the procedure.

Intracardiac Echocardiography

Our prototype catheter transducers were not fitted with mechanical steering mechanisms. To overcome this limitation, the *in vivo* images were acquired after surgery (median sternotomy or left thoracotomy) to expose the heart. Small incisions were made in the appropriate cardiac chambers to allow access of our imaging catheter. The incisions were then closed with a purse string suture. Use of the open chest model allowed us to confirm the locations, orientations and imaged structures in each experiment using manual palpation of the cardiac chambers, vessels and the catheters therein.

Results

Transducers

We have previously reported the spectrum of the 64 channel 5 MHz catheter transducer to have a -6 dB fractional bandwidth of 50% and a center frequency of 5.2 MHz.⁸ The 137 channel catheter has a -6 dB fractional bandwidth of 29% with a center frequency of 4.2 MHz.¹⁸ The 137 channel transducer does not have a matching layer, which accounts for the lower bandwidth.

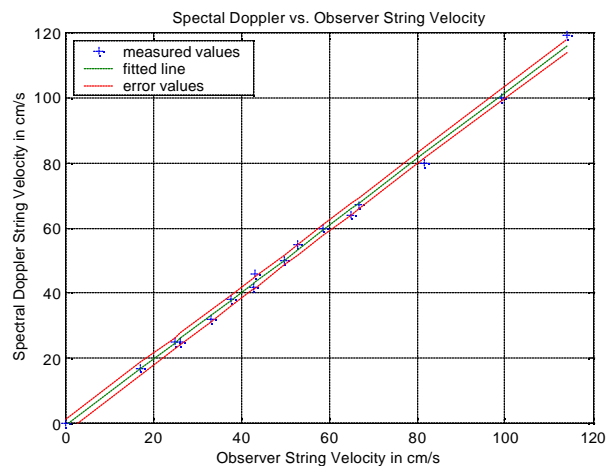


Figure 5. Plot of measured Spectral Doppler string velocity vs. observed results.

String phantom

The results from the measurements of the string phantom using SPECTRAL Doppler are shown in figure 5. The Spectral Doppler measurements are plotted vs. the observers'

measurements. The fitted line shows a slope of 1.024 and a Y intercept of -0.706. The calculated error has a mean value of 1.764.

Figure 6 shows the results measuring the string velocity using CF Doppler. The CF Doppler measurement are plotted vs. the observers' results. The fitted line shows a slope of 0.914 and a Y intercept of -8.365. The calculated error has a mean value of 2.955.

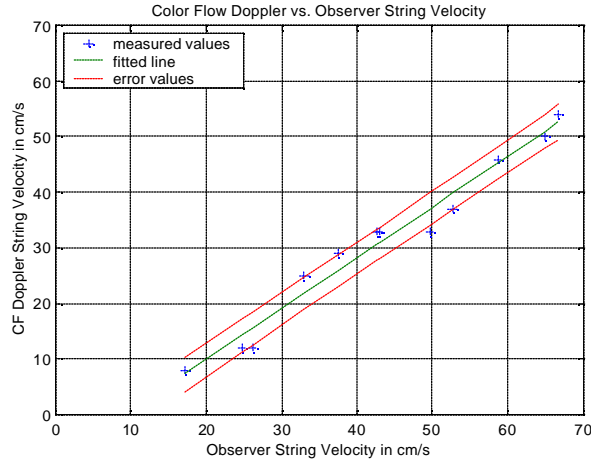


Figure 6. Plot of measured Color Flow Doppler string velocity vs. observed results.

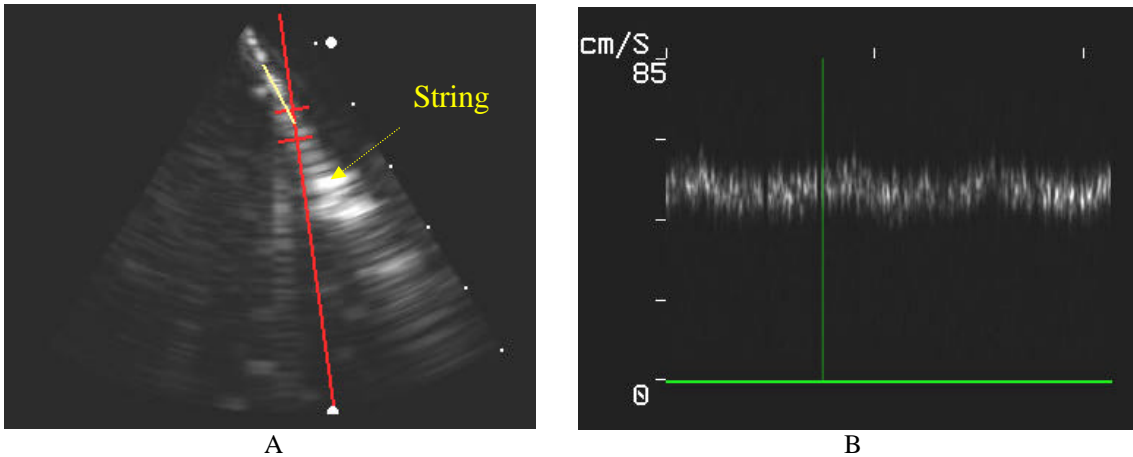


Figure 7. Spectral Doppler Flow of the string phantom. Figure 7A shows a 6 cm deep B-scan and the position of the Spectral marker (red) and the azimuthal angle correction (yellow). The arrow indicates the string. The Spectral Doppler in Figure 7B measures the velocity to be about 46 cm/s.

Figures 7 and 8 show typical Spectral Doppler and the Color Flow images of the string phantom, respectively. Figure 7A shows a 6 cm deep B-scan of the string and the location of the Spectral Doppler marker in red and the azimuthal angle correction in yellow. In figure 7B, the Spectral Doppler shows the string to be moving at a velocity of nearly 46 cm/s. Figure 8 shows a 6 cm deep B-scan/Color Flow image. Flow towards the transducer is colored in red to yellow. In figure 8A and the corresponding real time Color Flow C-scan in figure 8B, we clearly see the flow is toward the transducer.

Cardiac Jet Phantom

Figures 9 and 10 show B-Scan, Spectral and Color Flow Doppler images of our cardiac jet phantom, respectively. These images were made with the 64 channel, 12 French catheter. Figure 9A shows one B-scan of the orifice and the location of the Spectral Doppler marker. The B-scan is 6 cm deep. Figure 9B shows the Doppler spectrum indicating the maximum flow rate to be about 22 cm/s and clearly shows the pulsatile nature of the flow. In figure 10, the Color Flow images clearly indicate the direction of the flow. This is seen in the real time C-scans as well as the simultaneous B-scans.

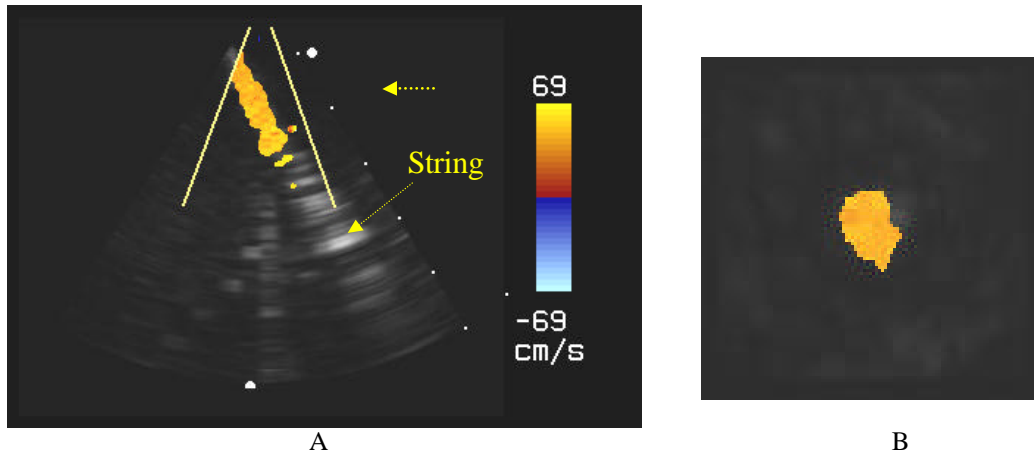


Figure 8. Color Flow Doppler image of the string phantom. Figure 8A shows the 6 cm deep B-scan and the Color Flow map indicating flow towards the transducers as yellow and away as blue. The green arrow shows the string in the image. Figure 8B shows the corresponding real time Color Flow C-scan at a depth indicated by the arrow in Figure 8A.

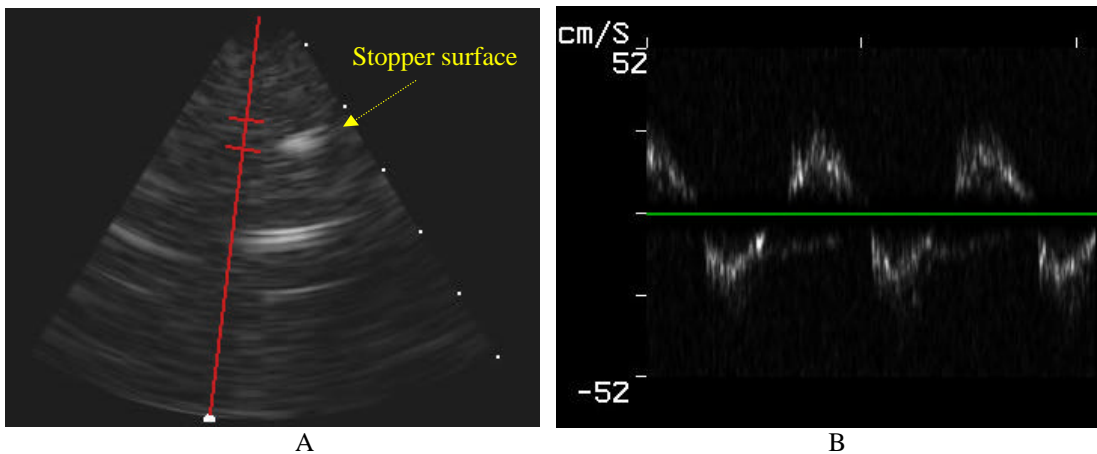


Figure 9. Spectral Doppler Flow of a cardiac jet phantom. Figure 9A shows the 6 cm deep B-scan with the marker. Figure 9B is the Spectral Doppler information showing the pulsatile flow and a maximum flow rate of 22 cm/s.

Discussion

We have extended our work with real time volumetric intracardiac imaging to include real time volumetric flow data. We have shown the same catheters used for 3D ICE can

also be used to acquire flow data in phantoms. From figure 5, we see that the Spectral Doppler gives an accurate prediction compared to the observers' results. The fitted line has a slope near 1, and a Y intercept close to 0. The Color Doppler can be used to qualitatively show flow, but not accurately predict it. The slope of the fitted line is good, but the large Y intercept shows that the technique constantly under-estimates the string velocity.

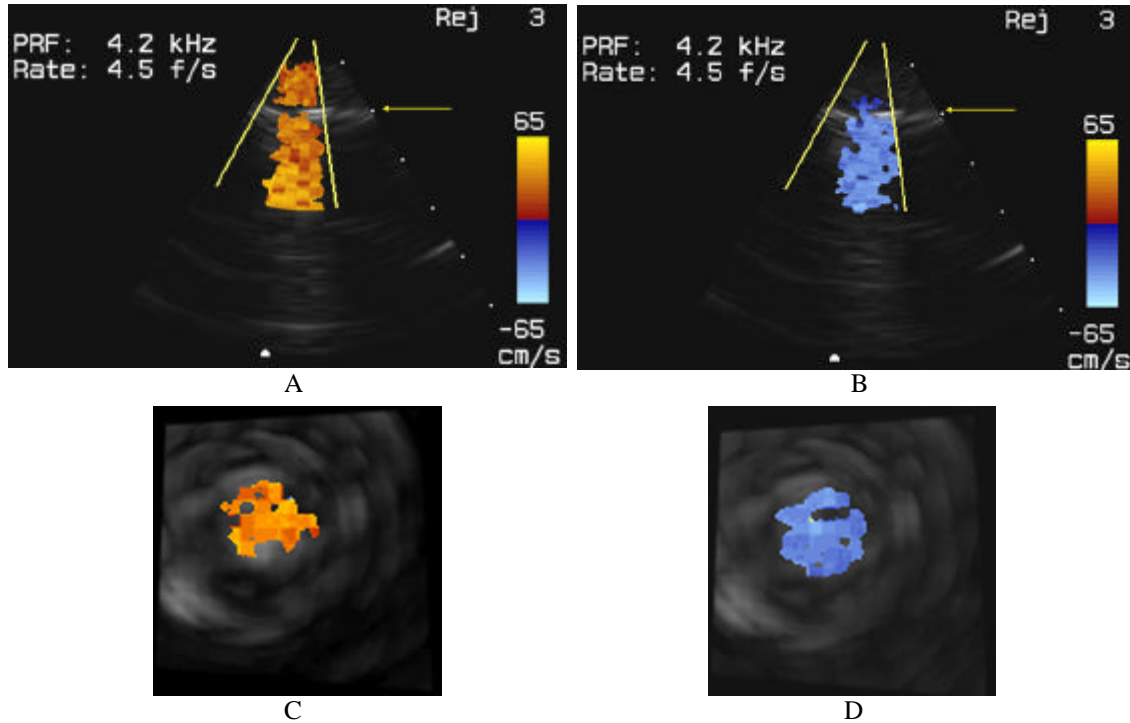


Figure 10. Color Doppler Flow of a cardiac jet phantom. The 6 cm deep B-scans show the flow moving towards (Fig. 10A) and away (Fig. 10B) from the transducer. The arrows indicate the location of the simultaneous real time C-scan planes shown in figures 10C and 10D.

We have not successfully shown *in vivo* flow. Figure 11 shows an attempt to obtain Spectral Doppler flow data in the aorta of the open chest sheep as imaged from the Superior Vena Cava. We used the 137 channel catheter transducer. Figure 11A shows the 6 cm deep B-scan with the location of the Spectral marker in the aorta. Figure 11B shows the resulting Spectral Doppler result. As the image shows, we can see the wall motion of the area near the valve complex, but we did not detect blood flow. We were also unable to obtain blood flow data with Color Doppler. Since other investigators have demonstrated blood flow with the Volumetrics system,¹⁴ this is a limitation of our transducers in combination with the imaging system. The imaging system is not designed to work with 5.0 MHz transducers. By injecting a swept frequency spectrum (Hewlett Packard Model 3588A Spectrum Analyzer) into the system, we measured the predetection system response at 5.0 MHz to be 15 dB below the peak at 1.75 MHz. The system also uses digital filtering in order to detect the Doppler signal. We used the Doppler filters that are designed for a 3.5 MHz array that comes with the system, but the bandwidths do not match the bandwidth of our transducers.

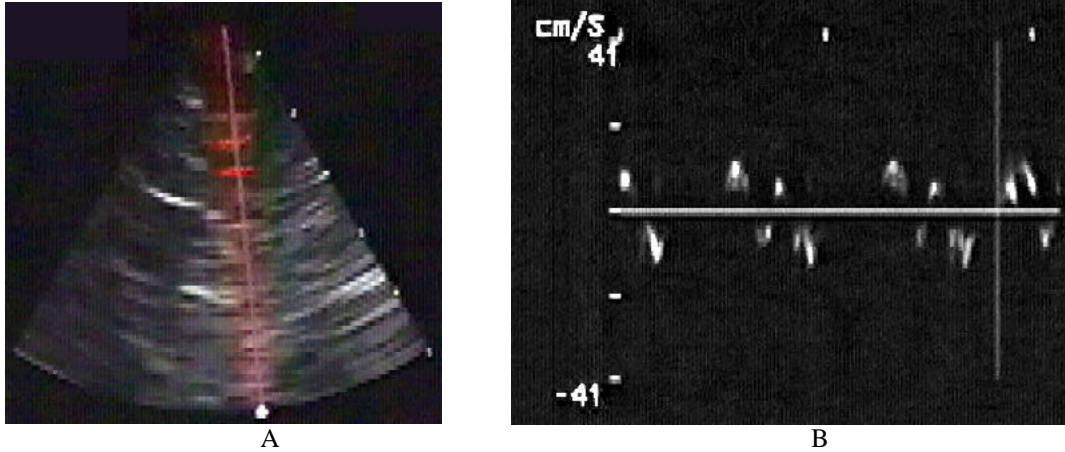


Figure 11. Spectral Doppler image showing wall motion in the aorta. Figure 11A shows the 6 cm deep B-scan and the location of the Spectral marker in red. Figure 11B shows the resulting Spectral Doppler.

While there are 137 available channels for the transducer, only 90 were working at the time of the study. This was due to failures in our flex circuits. There are yield problems as well as transducer processing difficulties with these flex circuits. We are working to obtain more robust flex circuits to improve our fabrication processes and to increase element yield. Finally, we note that the clinical transthoracic Doppler study used 2D array transducers of 256 transmitters and 256 receivers at 2.5 MHz which yielded a much improved signal to noise ratio compared to our catheter array transducer.

We need to improve the signal to noise ratio of our catheter transducers to image the blood and detect flow. In order to accomplish this, we need to develop transducers with more active elements and improved materials. To increase the number of active elements, we are pursuing new cabling technologies.^{18, 20} The 137 channel transducer did not have a matching layer. By adding a matching layer, we will improve the signal to noise ratio.

References

1. Kalman M.J., Olgin J.E., Karch M.R., and Lesh M.D., Use of intracardiac echocardiography in interventional electrophysiology, *Pacing and Clinical Electrophysiology* 22, pp. 2248-2262, 1997.
2. Bruce C.J., Packer D.L., Belohlavek M., Seward J.B., Intracardiac echocardiography: newest technology, *J Amer. Soc. Echocard.* 13, pp. 788-795, 2000.
3. Bruce, C. J., Packer, D.L. and Seward, J.B., Intracardiac Doppler hemodynamics and flow: new vector, phased-array ultrasound-tipped catheter, *Amer. J. Card.* 83, May 15 pp. 1509-1512, 1999.
4. von Ramm O.T. and Smith S.W., Real-time volumetric ultrasound imaging system", *J. Diag. Imag.* 3, pp. 261-266, 1990.
5. Smith, S.W., Pavy, H.E., and von Ramm, O.T., High speed ultrasound volumetric imaging system part I: transducer design and beam steering, *IEEE Trans. Ultras., Ferro. and Freq. Control* 38, pp. 100-108, 1991
6. von Ramm, O.T., Smith, S.W., and Pavy, H.E., High speed ultrasound volumetric imaging system part II: parallel processing and display, *IEEE Trans. Ultras., Ferro. and Freq. Control* 38, pp. 109-115, 1991

7. Light, E.D., Davidsen, R.E., Fiering, J.O., Hruschka, T.A., and Smith, S.W., Progress in two dimensional arrays for real time volumetric imaging, *Ultrason. Imag.* 20, no. 1, pp. 1-16, 1998.
8. Light, E.D., Fiering, J.O., Hultman, P.A., Lee, W., and Smith, S.W., Update of two dimensional arrays for real time volumetric and real time intracardiac imaging, *Proceedings IEEE Trans. Ultrason. Symp.*, pp. 1217-1220, IEEE cat. no. 99CH37027 (1999).
9. Light, E.D., Hultman, P.A., Idriss, S.F., Lee, W., Wolf, P.D. and Smith, S.W., Two dimensional arrays for real time volumetric and intracardiac imaging with simultaneous electrocardiogram, *Proc. IEEE Trans. Ultrason. Symp.*, pp. 1195-1198, IEEE cat. no. 00CH37121 (2000).
10. Schmidt M.A., Ohazama C.J., Agyeman K.O., et al., Real-time three-dimensional echocardiography for measurement of left ventricular volumes, *Amer. J. Card.* 84, pp. 1434-1439, 1999.
11. Qin JX, Jones M, Shiota T, Greenberg NL, et al., Validation of real-time three-dimensional echocardiography for quantifying left ventricular volumes in the presence of a left ventricular aneurysm: In vitro and *in vivo* studies, *J. Amer. Coll. Card.* 36, pp. 900-907, 2000.
12. Ahmad M., Xie T.R., McCulloch M., Abreo G., Runge M., Real-time three-dimensional dobutamine stress echocardiography in assessment of ischemia: Comparison with two-dimensional dobutamine stress echocardiography, *J. Amer. Coll. Card.* 37, pp. 1303-1309, 2001.
13. Firek, B., Higginbotham, M., Russel, S., et al., Initial experience with volume-rendered, real-time three dimensional echocardiography in right ventricular endomyocardial biopsy (abstract), *Eur. Heart J.* 21, pp. 3064, 2000.
14. Tsujino, H., Jones, M., Shiota, T., et al, Real-time three dimensional color Doppler echocardiography for characterizing the spatial velocity distribution and quantifying the peak flow rate in the left ventricular outflow tract, *Ultrasound in Med and Biol.* 27, No. 1, pp. 69-79, 2001.
15. Fiering, J.O., Hultman, P., Lee, W., Light, E.D. and Smith, S.W., High density flexible interconnect for two-dimensional ultrasound arrays, *IEEE Trans Ultras. Ferro and Freq. Control* 47, pp. 764-770, 2000.
16. Light, E.D., Idriss, S.F., Wolf, P.D. and Smith, S.W., Real Time 3D Intracardiac Echocardiography, *Ultrasound in Med and Biol.* 27, No. 9, pp. 1177-1183, 2001.
17. Smith, S.W., Light, E.D., Idriss, S.F. and Wolf, P.D., Feasibility study of real time three dimensional intracardiac echocardiography for guidance of interventional electrophysiology. *Pacing and Clinical Electrophysiology* 25, No. 3, pp. 351-357, 2002.
18. Lee, W., Light, E.D., Hultman, P.A., Idriss, S.F., Dixon-Tulloch, E., Wolf, P.D. and Smith, S.W., Real-time three dimensional intracardiac echocardiography for guidance of cardiac interventional procedures, *Proceedings IEEE Trans. Ultrason. Symp.*, pp. 1307-1310, IEEE cat. no. 01CH37263 (2001).
19. Guide to the Model 1, Volumetrics Medical Imaging, Durham, NC.
20. Griffith J. and Lebender R., Electrical characteristics of ribbon based probe cables, *Proc. IEEE Ultras. Symp.* 99CH37027, pp. 1085-1090, IEEE cat. no. 99CH37027 (1999).